British Journal of Pharmacology (2004) 142, 709–718
www.nature.com/bjp

Depolarization-induced calcium influx in rat mesenteric small arterioles is mediated exclusively *via* mibefradil-sensitive calcium channels

*,[1]Lars J. Jensen, [1]Max Salomonsson, [2]Boye L. Jensen & [1]Niels-Henrik Holstein-Rathlou

[1]Department of Medical Physiology, Division of Renal and Cardiovascular Research, The Panum Institute, University of Copenhagen, Copenhagen DK-2200, Denmark and [2]Department of Physiology and Pharmacology, Odense University, Odense DK-5000, Denmark

1 In this study, intracellular Ca^{2+} was measured as the Fura-2 ratio (R) of fluorescence excited at 340 and 380 nm (F_{340}/F_{380}) in nonpressurized rat mesenteric small arterioles ($\varnothing$ (lumen diameter) 10–25 μm). The response to depolarization using 75 mM KCl was an increase in R from a baseline of 0.96 ± 0.01 ($[Ca^{2+}]_i \sim 74$ nM) to 1.04 ± 0.01 (~ 128 nM) ($n = 80$).

2 The response to 75 mM K^+ was reversibly abolished in Ca^{2+}-free physiological saline solution, whereas phentolamine (10 μM) or tetrodotoxin (1 μM) had no effects. $LaCl_3$ (200 μM) inhibited $61 \pm 9\%$ of the response.

3 A [K^+]-response curve indicated that the Ca^{2+} response was activated between 15 and 25 mM K^+. The data suggest that the Ca^{2+} response was caused by the activation of voltage-dependent Ca^{2+} channels.

4 Mibefradil use dependently inhibited the Ca^{2+} response to 75 mM K^+ by $29 \pm 2\%$ (100 nM), $73 \pm 7\%$ (1 μM) or $89 \pm 7\%$ (10 μM). Pimozide (500 nM) use dependently inhibited the Ca^{2+} response by $85 \pm 1\%$.

5 Nifedipine (1 μM) inhibited the Ca^{2+} response to 75 mM K^+ by $41 \pm 12\%$. The response was not inhibited by calciseptine (500 nM), ω-agatoxin IVA (100 nM), ω-conotoxin MVIIA (500 nM), or SNX-482 (100 nM).

6 Using reverse transcriptase–polymerase chain reaction, it was shown that neither $Ca_V2.1a$ (P-type) nor $Ca_V2.1b$ (Q-type) voltage-dependent Ca^{2+} channels were expressed in mesenteric arterioles, whereas the $Ca_V3.1$ (T-type) channel was expressed. Furthermore, no amplification products were detected when using specific primers for the β_{1b}, β_2, or β_3 auxiliary subunits of high-voltage-activated Ca^{2+} channels.

7 The results suggest that the voltage-dependent Ca^{2+} channel activated by sustained depolarization in mesenteric arterioles does not classify as any of the high-voltage-activated channels (L-, P/Q-, N-, or R-type), but is likely to be a T-type channel. The possibility that the sustained Ca^{2+} influx observed was the result of a T-type window current is discussed.
British Journal of Pharmacology (2004) **142,** 709–718. doi:10.1038/sj.bjp.0705841

Keywords: Microcirculation; resistance vessel; arteriole; vascular smooth muscle cell; voltage-dependent Ca^{2+} channel; conducted vascular response; mibefradil; pimozide; calciseptine; use dependence

Abbreviations: EGTA, ethylene glycol-*bis*(2-aminoethylether)-*N*,*N*,*N*′,*N*′-tetraacetic acid; NMDG, *N*-Methyl-D-glucosamine; NO, nitric oxide; PSS, physiological saline solution; TTX, tetrodotoxin; V_m, membrane potential; VSMC, vascular smooth muscle cell; $\varnothing$, lumen diameter

Introduction

Voltage-dependent Ca^{2+} channels are crucial for excitation–contraction coupling in muscle cells from the heart, skeletal muscle and various types of smooth muscle including vascular smooth muscle cells (VSMC). These channels have been roughly divided into high-voltage-activated (L-, P/Q-, N-, R-type) vs low-voltage-activated calcium channels (T-type) (Hofmann *et al*., 1999), referring to the fact that the former requires larger depolarization for activation than the latter.

In the majority of VSMC, excitation–contraction coupling is maintained by L-type Ca^{2+} channels pharmacologically distinguished by their sensitivity to dihydropyridines such as nifedipine (McDonald *et al*., 1994; Perez-Reyes, 2003). However, in microvascular resistance vessels other types of voltage-dependent Ca^{2+} channels have emerged that were previously believed to function only in the heart or brain tissue. In rat cremaster muscle arterioles, T-type Ca^{2+} channels are involved in the maintenance of vascular tone (VanBavel *et al*., 2002), and in renal afferent arterioles from rabbit or rat, both T-type (Hansen *et al*., 2001) and P/Q-type (Hansen *et al*., 2000) channels appear to have a functional role in depolarization-induced vasoconstriction and Ca^{2+} influx. Furthermore, in a recent study, we demonstrated that mRNA coding for the pore-forming α_{1C}-subunit ($Ca_V1.2$) of the L-type

*Author for correspondence; E-mail: ljj@mfi.ku.dk
Advance online publication: 1 June 2004

Ca^{2+} channel was absent in rat mesenteric arterioles, whereas that of α_{1G}- ($Ca_V3.1$) and α_{1H}- ($Ca_V3.2$) subunits of the T-type Ca^{2+} channel were expressed (Gustafsson *et al*., 2001). In addition, vasoconstriction in rat mesenteric arterioles (∅ (lumen diameter) $<40\,\mu$m) *in vivo* appeared to rely on mibefradil-sensitive and dihydropyridine-insensitive Ca^{2+} channels (Gustafsson *et al*., 2001).

In agreement with the above findings, isolated smooth muscle cells from rat and guinea-pig mesenteric artery terminal branches (∅ 50–100 μm) displayed nifedipine-insensitive, voltage-activated Ca^{2+} currents with T-channel-like pharmacological properties (Morita *et al*., 2002). However, the biophysical properties of this channel were different from 'classical' low voltage-activated T-type channels (Morita *et al*., 1999). The major difference to T-type characteristics were activation at more depolarized potentials (threshold at -50 to -40 mV and peak current at -15 to -10 mV) than typical T-type currents with activation threshold at -70 to -60 mV and peak current at -40 to -30 mV. Moreover, physical ion pore properties (Ba^{2+}/Ca^{2+} permeability; Cd^{2+}/Ni^{2+} blocking efficacy) suggested that this channel belongs to the class of high-voltage activated Ca^{2+} channels (e.g. R-type), rather than low-voltage activated (T-type) channels (Morita *et al*., 1999; 2002). These authors therefore suggested that this channel is either a novel type of voltage-activated Ca^{2+} channel with mixed properties known from R- and T-type channels or an alternative splice variant of the T-type channel.

Owing to the fast inactivating nature of native T-type channels (τ_{inact} 5–50 ms), they have been thought to play little role in Ca^{2+} influx during sustained depolarization. However, small steady-state Ca^{2+} currents occurring in the voltage 'window' between overlapping steady-state activation and inactivation curves (window currents) may account for sustained Ca^{2+} influx into cells (McDonald *et al*., 1994; Morita *et al*., 1999; Perez-Reyes, 2003). A physiological role for T-type window currents has recently been demonstrated in human myoblast terminal differentiation where they mediated the sustained Ca^{2+} entry required for myoblast fusion (Bijlenga *et al*., 2000).

In the present study, we have characterized the pharmacological properties of depolarization-induced Ca^{2+} influx in isolated rat mesenteric small arterioles (∅ 10–25 μm) stimulated by elevated bath K^+ concentration. The induced Ca^{2+} increases are hypothesized to rely on window currents through Ca^{2+} channels that display fast voltage-dependent inactivation (T-type). Using reverse transcriptase–polymerase chain reaction (RT–PCR), we have also investigated the mRNA expression profile of a selection of known α_1- (pore-forming) and β-(auxiliary) subunits of voltage-dependent Ca^{2+} channels.

Methods

Animals and microdissection of mesenteric arterioles

A total of 51 male Wistar rats (age 7–10 weeks; weight 261 ± 24 g) were anesthetized by inhalation of 2–5% halothane or sevofluran in a mixture of 35% O_2 with 65% N_2. A catheter was inserted in the left jugular vein for infusion and a tracheal catheter was used to secure free airways. At this point, halothane/sevofluran anesthesia was stopped and a continuous intravenous infusion of pentobarbital sodium (154 μg min^{-1}) initiated.

A median laparotomy was performed and a loop of the small intestine with adjacent mesentery was pinned onto Sylgard® covering the bottom of a Petri dish filled with isotonic NaCl kept at room temperature. The mesenteric microcirculation was examined with a Leica Wild M10 stereomicroscope ($\times 8-63$ magnification). The arterioles (resistance vessels) of interest derive from first- or second-order branches of the superior mesenteric artery and give rise to capillary networks supplying the mesentery. The criteria for selection of arterioles (∅ 10–25 μm) branching from an artery into the transparent part of the mesentery were observation of a fast pulsating blood flow and that they gave rise to smaller capillaries downstream of the point of observation. Arterioles with surrounding tissue were isolated and transferred onto a glass beaker containing ice-cold physiological saline solution (PSS) with 1% bovine serum albumin (BSA). With the aid of a microscope ($\times 95$), microdissection was carried out in a glass dish placed in an ice-cold metal block. Each arteriole was dissected free from fat and as much of the surrounding tissue as possible while avoiding stretching or damaging the vessel.

RNA isolation, RT–PCR and Southern blotting

A total of 4–6 mm arteriole (∅ 10–25 μm) per rat ($n=2$) was microdissected and transferred onto an Eppendorf tube (on ice) containing 400 μl RLT buffer (Qiagen, Germany) and freshly added β-mercaptoethanol (1%).

Arterioles were added directly to guanidinium thiocyanate (4 mol l^{-1}). For homogenization, the fragments were repeatedly triturated through syringes with decreasing dimension ending with 25 G. Yeast tRNA (12 μg) was added as carrier. Total RNA was extracted by phenol–chloroform extraction, precipitated with isopropanol and repeatedly washed with 70% ethanol (Andreasen *et al*., 2000). RNA pellets were suspended in diethyl pyrocarbonate water and used for cDNA synthesis as previously described in detail (Andreasen *et al*., 2000).

PCRs were performed with DNA oligonucleotides (Invitrogen) for rat $Ca_V2.1$, $Ca_V3.1$, smooth muscle auxiliary β_3-subunit, cardiac β_2-subunit, or neuronal β_{1b}-subunit. β-actin primers and reaction components were as described previously (Andreasen *et al*., 2000). As negative control, reverse transcription of total RNA was carried out in the absence of reverse transcriptase and subsequently amplified by PCR. As positive control for PCR, cDNA (50 ng) synthesized from various rat organs (cerebral cortex, left cardiac ventricle, and renal inner medulla) was used.

A dual set of PCR primers was designed to distinguish between $Ca_V2.1a$ (P-type) and $Ca_V2.1b$ (Q-type) at the splice site determining the ω-agatoxin IVA affinity, namely, the N1605-P1606 insertion. One forward primer was designed to hybridize upstream from the splice site. Two reverse primers were designed to overlap the splice site in such a way that each reverse primer would hybridize only to the chosen splice variant. All PCR products were verified by sequencing. Sequences were read on an ABI Prism genetic analyzer using ready-reaction mix from ABI, and templates were PCR products or on subcloned PCR products (plasmid pSP73, Promega).

- $Ca_V2.1a$ sense primer: 5′-gcc ctt cga gtg ttc aac-3′; antisense $Ca_V2.1a$: 5′-ctc agg ttg atg aag tta ttc c-3′, covering bases 4642–4826, 185 bp.
- $Ca_V2.1b$ sense primer: 5′-cag gtt gat gaa gtt att cgg-3′ (covering bases 4642–4824 + 6 bp), 189 bp. GenBank accession no. M64373 (Bourinet *et al*., 1999).
- $Ca_V3.1$ sense primer: 5′-gaa cgt gag gcc aag agt-3′; antisense: 5′-gct tgt atg cgt tcc cct-3′, covering bases 3910–4130, 221 bp. GenBank accession no. AF027984 (Andreasen *et al*., 2000).
- β_{1b} (neuronal) sense primer: 5′-tgt caa act gga cag c; antisense: 5′-aag aag tca aac aac gcc, 282 bp. GenBank accession no. X61394.
- β_2 (cardiac) sense primer: 5′-gga gga aat tca tca tcc; antisense: 5′-ttc cgc taa gct cga cc, 459 bp. GenBank accession no. 0M80545.
- β_3 (smooth muscle) sense primer: 5′-caa aca gga aca gaa gg; antisense: 5′-gat ggt cct ctt gcc, 324 bp. GenBank accession no. M88751.

RT–PCR was performed with annealing temperature between 50 and 60°C for 32–33 cycles (Eppendorf, Mastercycler).

Ca^{2+} indicator loading and intracellular Ca^{2+} measurements

Microdissected arterioles were transferred onto a glass dish containing PSS-based loading buffer to which Fura-2/AM had been added, and loaded for 120 min at room temperature in the dark. Alternatively, vessels were glued onto the cover slide bottom of the recording/perfusion chamber (Warner Instrument, Inc., CT, U.S.A.) using Cell-Tak (Becton Dickinson Labware, MA, U.S.A.), and incubated with Fura-2 herein under similar conditions. Following loading, the vessels were rinsed with fresh PSS, mounted between two suction pipettes (tip o.d. $\sim 20\,\mu$m) if not already immobilized using Cell-Tak, and rested for 20–30 min before performing measurements. There was no difference between results obtained with arterioles immobilized using Cell-Tak or suction pipettes.

The recording chamber (~ 0.1 ml capacity) was mounted onto the stage of an inverted fluorescence microscope (Olympus IX50). Solutions were added *via* a continuous superfusion flow ($\sim 1.7\,\text{ml}\,\text{min}^{-1}$) and excess solution was removed by suction. A quartz oil-immersion objective (Olympus $\times 40/1.35$) was used for Ca^{2+} measurements and the nonpressurized arterioles were visualized (see Figure 1) on a PC monitor using a digital video camera (SensiCam) and the Image Workbench (Axon) software package. Using a monochromator controlled by the software, the preparation was excited with fluorescent light of alternating wavelengths (340 vs 380 nm). A region of interest (ROI) for the measurement of intracellular calcium concentration ($[Ca^{2+}]_i$) was selected using a software routine. The fluorescence emitted in the ROI was detected by the digital camera and stored to a PC hard disk. Results are expressed as the Fura-2 ratio ($R = F_{340}/F_{380}$), which was calculated after a constant background signal had been subtracted from each wavelength. $[Ca^{2+}]_i$ was calculated using the Grynkiewics equation (Grynkiewicz *et al*., 1985):

$$[Ca^{2+}]_i = K_d \left[\frac{(R - R_{min})}{(R_{max} - R)}\right]\left[\frac{(F_{min,380})}{(F_{max,380})}\right]$$

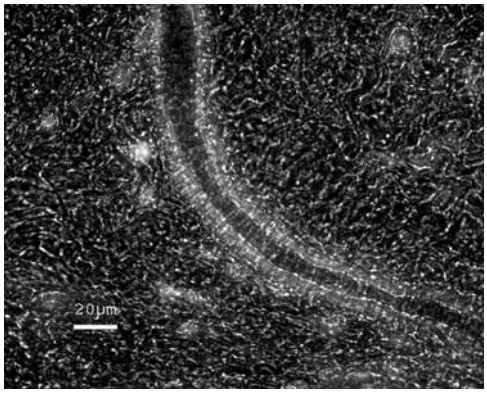

Figure 1 Micrograph of Fura-2-loaded arteriole in isolated rat mesentery. The tissue was excited at 340 nm and emission collected at 510 nm, giving rise to the bright fluorescence seen in the arteriolar wall. For the purpose of illustration, a dimmed transmission light was used to distinguish the arteriolar lumen and wall from the mesenteric tissue. The few bright spots seen in the mesentery probably correspond to fibroblasts loaded with Fura-2. The freshly isolated tissue was glued to a cover slide and subsequently loaded with Fura-2/AM in the recording chamber. In some cases, excess mesenteric tissue was carefully removed by microdissection prior to Fura loading and arterioles mounted between two suction pipettes during recordings.

Here, K_d is the Fura-2 dissociation constant for Ca^{2+}, R is the ratio of emitted fluorescence (F) at 340 over 380 nm, min and max denotes values obtained with Ca^{2+}-free solution or a solution with saturating $[Ca^{2+}]$, respectively. The K_d value used was 227 nM and K_d, R_{min}, R_{max}, $F_{min,380}$, and $F_{max,380}$ were determined *in vitro* using commercially available calibration buffers and Fura-2 pentapotassium salt (Molecular Probes, Leiden, The Netherlands).

Prior to experimentation, arterioles were rejected if the background-subtracted fluorescence of the adjacent tissue was $>50\%$ of that observed in arterioles or if changes in flow rate or solution level caused excess noise. Less than 5% of arterioles were rejected due to the lack of a Ca^{2+} response to 75 mM K^+. In acceptable preparations, a stable baseline measurement of 1–2 min was recorded before any stimulus was applied.

In most of the experiments, arterioles were superfused two to four times with high-K^+ solution for 40–100 s and with 2 min intervals. Subsequently, arterioles were exposed to an experimental drug dissolved in normal PSS for 1–5 min before the high-K^+ solution was applied two to four times in the presence of the same drug. A washout and resting period of 2–3 min was followed by two to four times high-K^+ stimulation in the absence of any drugs. In neurotoxin experiments, solutions were added by pipette (>20 times the bath volume) instead of by superfusion to reduce the amount of toxin needed. There was no difference between basal high-K^+ responses obtained with the protocol for neurotoxin experiments compared to that used in the remainder of the study.

Solutions and chemicals

PSS contained (in mM): 140 NaCl, 6 KCl, 1 $MgCl_2$, 1.8 $CaCl_2$, 5 *N*-(2-hydroxyethyl)piperazine-*N*′-(2-ethanesulfonic acid; 4-(2-hydroxyethyl)piperazine-1-ethanesulfonic acid (HEPES), and 5 glucose, with pH adjusted to 7.4. In solutions with elevated $[K^+]$ (high-K^+ PSS), NaCl was substituted with

equimolar amounts of KCl. In calcium-free PSS, $CaCl_2$ was substituted with 1 mM ethylene glycol-*bis*(2-aminoethylether)-*N*,*N*,*N*′,*N*′-tetraacetic acid (EGTA). In Na^+-free PSS, NaCl was substituted mole for mole with *N*-Methyl-D-glucosamine chloride (NMDG-Cl). The loading buffer consisted of 5 μM Fura-2/AM (Molecular Probes), 1% BSA, 0.5% DMSO, 0.02% Pluronic F127, 0.06% Cremophore EL, and 2.5 mM Probenecid (all from Sigma-Aldrich, Steinheim, Germany) dissolved in PSS.Mibefradil (F. Hoffmann-La Roche Ltd, Basel, Switzerland), $LaCl_3$, phentolamine (both Sigma-Aldrich, Steinheim, Germany), calciseptine, ω-agatoxin IVA, ω-conotoxin MVIIA, SNX-482, and tetrodotoxin (TTX) (all Alomone Labs, Jerusalem, Israel) were added from stock solutions prepared from water. Nifedipine and pimozide (both Sigma-Aldrich, Steinheim, Germany) were dissolved in DMSO, which was finally diluted to 0.001–0.005% in PSS. In vehicle control experiments, there were no effects of 0.005% DMSO alone ($n=4$).

Data presentation and statistics

Baseline Ca^{2+} measurements were reported as crude ratios or means$\pm$s.e. of the ratio, and in addition global mean values were reported as approximate $[Ca^{2+}]_i$ values. Calcium responses to high K^+ were summarized as % of baseline $R(100\times R_{stim}/R_{bas})$, and calcium responses during drug application were summarized as % inhibition $(100-(100\times\Delta R_{drug}/\Delta R_{ctr}))$. Statistical tests were paired Student's *t*-tests (unless otherwise stated), two-sided, and performed at the 5% level of significance. In cases where use of a nonparametric test is indicated, the data could not pass the test for normality.

Results

Ca^{2+} measurements under resting and stimulated conditions (high $[K^+]$)

In a total of 80 arterioles from 51 rats the baseline Fura-2 ratio was 0.96 ± 0.01, corresponding to a global mean resting $[Ca^{2+}]_i$ of $\sim$74 nM. Superfusing arterioles with PSS containing 75 mM K^+ instead of 6 mM resulted in an increase in the ratio from the resting level to 1.04 ± 0.01 ($P<0.001$, signed-rank test) or 108 ± 1% of the baseline value (see Figure 2a and b). The response to 75 mM K^+ corresponds to a $[Ca^{2+}]_i$ increase of approximately 54 nM from $\sim$74 to $\sim$128 nM.

Ca^{2+} entry vs mobilization

The calcium response to high K^+ could in principle be induced by depolarization of nerve terminals, thereby causing release of neurotransmitters such as noradrenaline, which would lead to receptor-mediated calcium mobilization in arterioles. To verify that this was not the case, the effect of the nonspecific α-adrenergic antagonist phentolamine and the neuronal voltage-dependent Na^+ channel blocker TTX was investigated. There was no significant difference between the high-K^+ response in the absence or presence of 10 μM phentolamine or with 1 μM TTX added to the phentolamine (Figure 2b).

To investigate the Ca^{2+} dependence of the response, arterioles were superfused with a Ca^{2+}-free PSS including a Ca^{2+} chelator (EGTA). As opposed to the control response in the presence of extracellular Ca^{2+}, the high-K^+ response was completely and reversibly abolished in Ca^{2+}-free PSS, indicating that the response was strictly dependent on calcium entry (see Figure 2a and b).

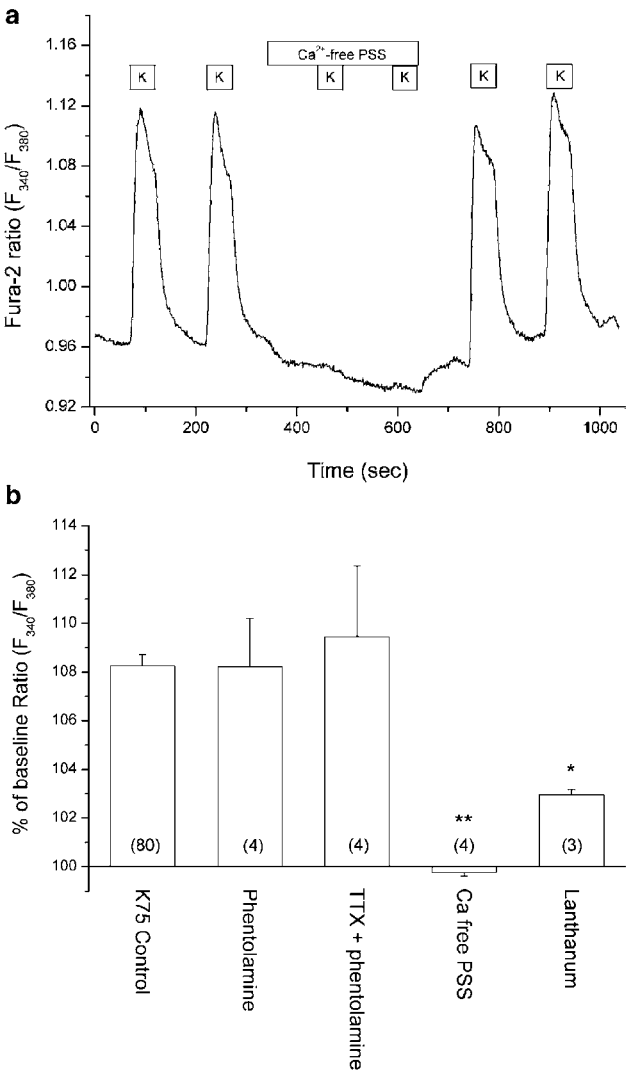

Figure 2 (a) Original recording of Fura-2 ratio (F_{340}/F_{380}) in mesenteric arteriole. Sustained depolarization induced by 75 mM K^+ (K) resulted in an increase of intracellular $[Ca^{2+}]$ (F_{340}/F_{380}) from the baseline level. The Ca^{2+} response was reversibly abolished in the presence of Ca^{2+}-free PSS with Ca^{2+} chelator (EGTA). (b) Summary of Ca^{2+} responses to 75 mM K^+ shown as % of baseline Fura-2 ratio. Compared to the control stimulation (K75 Control), the Ca^{2+} response was not altered by treatment with phentolamine (10 μM) or addition of TTX (1 μM) on top of phentolamine. However, the response was partially blocked in the presence of 200 μM La^{3+}. The number of arterioles used is shown within parenthesis. $*P<0.05$, $**P<0.01$; *t*-test vs control stimulation.

Trivalent metal ions (e.g. La^{3+}) have been used to block currents through transiently expressed voltage-activated Ca^{2+} channels (Beedle *et al*., 2002). In the present study, we used lanthanum ($LaCl_3$) to test whether the calcium influx was sensitive to trivalent metal ions. The response to high K^+ was reversibly reduced in the presence of 200 μM La^{3+}, corresponding to an inhibition of 61 ± 9%.

A dose–peak response relationship was obtained for elevated extracellular K^+ concentrations of 15, 25, 50, 75,

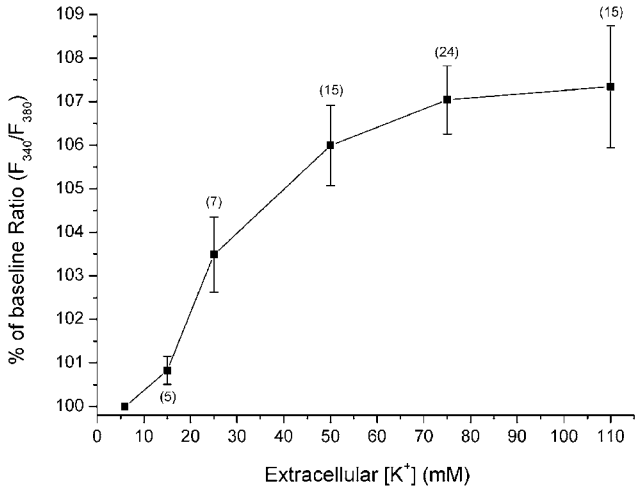

Figure 3 In a number of unpaired experiments, arterioles were subjected to depolarization with varying extracellular [K^+]. The concentration–peak response curve indicates activation of Ca^{2+} entry between 15 and 25 mM extracellular K^+ and the response is maximal at approximately 75 mM K^+. The number of arterioles used is shown within parenthesis.

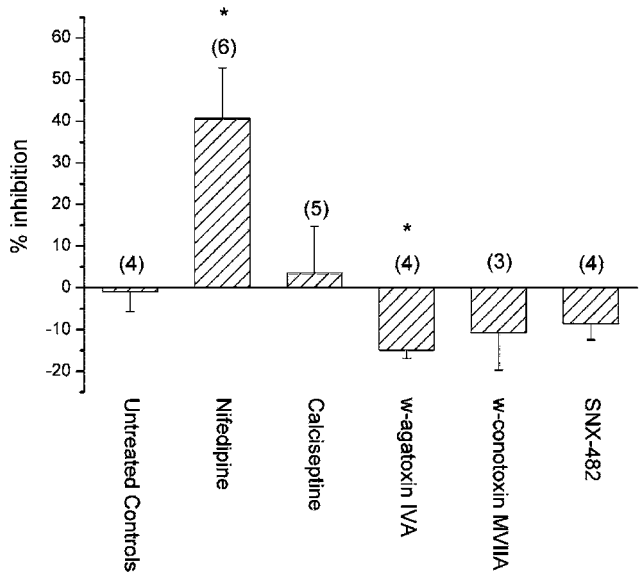

Figure 4 Effects of various Ca^{2+} channel blockers shown as % inhibition of the Ca^{2+} response to 75 mM K^+. The L-type Ca^{2+} channel blocker nifedipine (1 μM) inhibited 40% of the response, whereas there was no effect of a highly specific L-type blocker, the neurotoxin calciseptine (500 nM). Highly specific neurotoxin blockers of P/Q-type (ω-agatoxin IVA, 100 nM), N-type (ω-conotoxin MVIIA, 500 nM), or R-type Ca^{2+} channels (SNX-482, 100 nM) did not inhibit the response to high K^+. There was a minor increase of the Ca^{2+} response in the presence of ω-agatoxin IVA. The number of arterioles is within parenthesis. $*P<0.05$; *t*-test vs untreated control experiments.

and 110 mM (Figure 3). The calcium response was activated between 15 and 25 mM K^+ and it was maximal at 75–110 mM K^+. The above data suggest that the high-K^+-induced Ca^{2+} response was mediated by voltage-dependent Ca^{2+} channels in the arteriolar wall.

Pharmacological characterization of the influx pathway

Effect of L-type blockers Our previous investigation (Gustafsson *et al*., 2001) revealed that rat mesenteric arterioles do not possess mRNA coding for the $Ca_V1.2$ α_1-subunit of the L-type Ca^{2+} channel, and in addition vasoconstriction *in vivo* was insensitive to dihydropyridines (10 μM nifedipine or nimodipine). To confirm these results, we tested the effect of nifedipine (1 μM) on the Ca^{2+} response to high-K^+ stimulation. Nifedipine induced a variable block from 0 to 70% inhibition (Figure 4). As this could be a nonspecific effect of nifedipine, we also tested the venom neurotoxin calciseptine reported to be a potent blocker of L-type Ca^{2+} channels with little or no effect on N- or T-type voltage-dependent Ca^{2+} channels (de Weille *et al*., 1991). In five mesenteric arterioles, 500 nM calciseptine did not inhibit the Ca^{2+} response to high K^+ (Figure 4), indicating that L-type channels do not play a role in this response and that the effect of nifedipine was nonspecific. To verify the efficacy of calciseptine, we tested its effect in freshly isolated rat renal afferent arterioles known to contain L-type Ca^{2+} channels (Salomonsson & Arendshorst, 1999; Loutzenhiser & Loutzenhiser, 2000). Using the same protocol as for mesenteric arterioles, 500 nM calciseptine induced a 47 ± 4% inhibition of the Ca^{2+} response to 75 mM K^+ in afferent arterioles ($P<0.01$, $n=4$).

Effect of P/Q-, N- and R-type blockers Functional evidence for P/Q-type Ca^{2+} channels and mRNA expression of the $Ca_V2.1$ α_1-subunit of this channel has recently been described in afferent arterioles from rat kidney (Hansen *et al*., 2000). We therefore tested the effect of the venom neurotoxin ω-agatoxin IVA, which is a specific blocker of P/Q-type Ca^{2+} channels (Mintz *et al*., 1992). In a total of four experiments, 100 nM ω-agatoxin IVA did not inhibit high-K^+-induced Ca^{2+} response in rat mesenteric arterioles, but instead induced a small, reversible, and significant increase (Figure 4). Specific neurotoxin blockers also exist for N-type (Feng *et al*., 2003) and R-type Ca^{2+} channels (Newcomb *et al*., 1998). There were no effects of the N-type blocker ω-conotoxin MVIIA (500 nM) or the R-type blocker SNX-482 (100 nM) (Figure 4).

Effect of mibefradil A recent study on rat mesenteric arterioles indicated a role for dihydropyridine-insensitive, mibefradil-sensitive Ca^{2+} channels (Gustafsson *et al*., 2001). We therefore tested the effects of mibefradil, which is known to inhibit T-type Ca^{2+} channels at submicromolar concentrations, whereas L-type channels are affected at micromolar concentrations. To exploit the use-dependent effects of mibefradil, we applied a protocol in which four brief (40 s) stimulations with 75 mM K^+ were followed by four stimulations in the presence of the drug to facilitate binding to channels in the open or inactivated state. Mibefradil did not change the baseline Fura-2 ratio, but it inhibited the response to high-K^+ (Figure 5a). Throughout the concentration range from 100 nM to 10 μM, there was a difference between the initial and fourth high-K^+ response in the presence of drug, indicating use dependence of mibefradil block (Figure 5b). This effect was time independent since there was no difference between responses obtained with 1, 3, or 5 min preincubation with mibefradil (data not shown). Using one-way repeated measures ANOVA with Student–Newman–Keuls *post hoc* test, there was a significant difference between the first vs the third and fourth high-K^+ stimulation in the presence of mibefradil

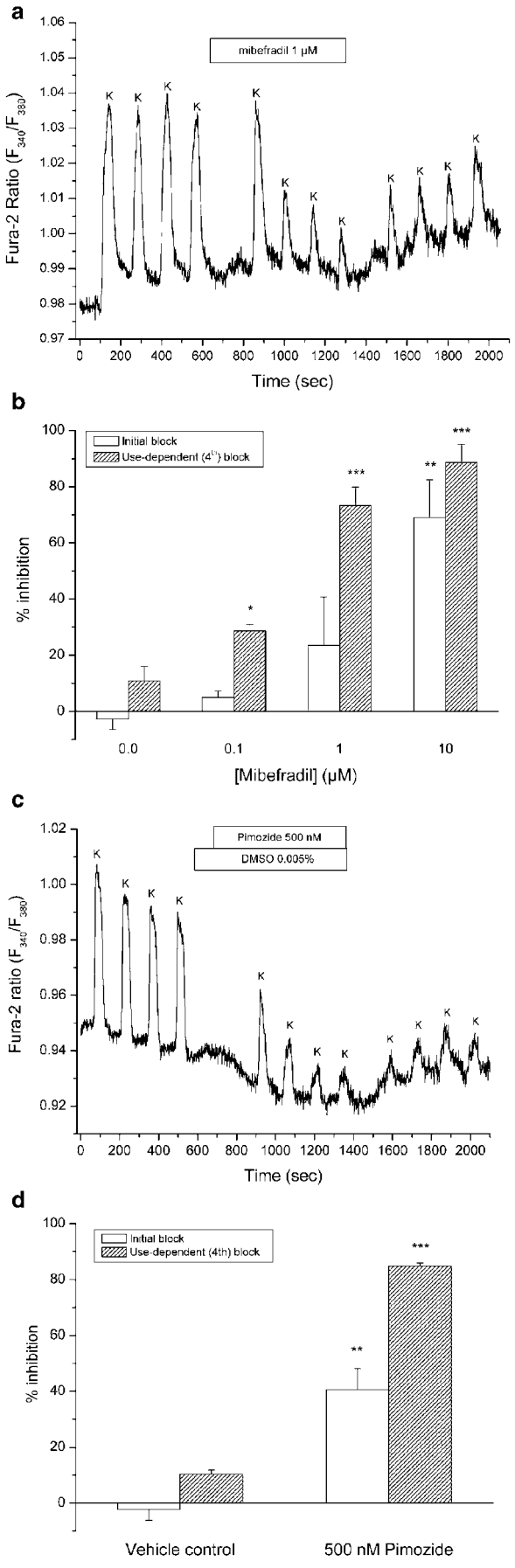

at both 100 nM ($P<0.001$, $n=4$) and 1 μM ($P<0.05$, $n=5$), but not at 10 μM ($n=4$). This difference was not detected in the untreated controls ($n=4$). A summary of % inhibition by dose level is presented in Figure 5b. Importantly, the use-dependent block induced by 100 nM mibefradil, a concentration believed to be specific for T-type channels, was statistically significant.

Effect of pimozide The neuroleptic agent pimozide is, apart from being a D_2 dopamine receptor antagonist, an effective blocker of voltage-dependent calcium channels (Enyeart *et al.*, 1990; 1993; Sah & Bean, 1994). In analogy with mibefradil, block of calcium channels by pimozide appears to be use dependent (Arnoult *et al.*, 1998). The use-dependent effect of pimozide was therefore investigated using the same protocol as for mibefradil (Figure 5c). In four arterioles, pimozide (500 nM) efficiently and use dependently blocked 85% of the calcium response to 75 mM K^+, whereas a slight inhibition (10%) was observed in the vehicle control experiments (Figure 5d). It should be noted that the baseline Fura-2 ratio was reversibly decreased from 0.965 ± 0.009 to 0.959 ± 0.010 after adding 500 nM pimozide. In vehicle control experiments, there was no change of the baseline ratio before compared to 1 min after adding 0.005% DMSO to the perfusate.

Activation of reverse mode Na^+/Ca^{2+} exchanger

With Na^+ as the major cation in the superfusate, the only way to increase bath [K^+] at a constant osmolarity is to substitute equimolar amounts of Na^+ in the bath. Depolarization of the cell and a concomitant lowering of the bath [Na^+] might reverse the electrogenic Na^+/Ca^{2+} exchanger that functions as a Ca^{2+} extrusion mechanism under control conditions. We investigated the effect of mibefradil on the Ca^{2+} response to bath Na^+ substitution with NMDG, as such an effect might compromise our conclusions with regard to mibefradil's effect on voltage-dependent Ca^{2+} channels. When bath Na^+ was substituted, a slowly activating ($t_{1/2}=41.8\pm10.5$ s) sustained increase of the Fura-2 ratio was observed from a baseline of 1.01 ± 0.04 to 1.36 ± 0.15 ($P=0.051$, $n=5$), corresponding to an approximate increase in $[Ca^{2+}]_i$ from $\sim$106 to $\sim$352 nM. There was no effect of 1 μM mibefradil on this response (4.7 ± 10.5% inhibition, $n=5$).

Figure 5 Effects of the T-type Ca^{2+} channel blockers mibefradil and pimozide. (a) In this original trace, an arteriole was stimulated repeatedly (12 stimulations of 40 s duration) with 75 mM K^+ (K). After four stimulations mibefradil (1 μM) was applied for a total period of $\sim$10 min. The inhibition induced by mibefradil was maximal after three to four stimulations, and this time-independent effect is referred to as use-dependent block. (b) Open columns depict % inhibition of the first stimulation (initial block) and hatched columns depict inhibition of the last stimulation (use-dependent block) in the presence of mibefradil at all concentrations tested ($n=4-5$). The untreated control experiments are shown here as 0.0 μM mibefradil ($n=4$). (c) Ca^{2+} responses to 75 mM K^+ (K) in an arteriole exposed to 500 nM of the antipsychotic pimozide, clearly showing a use-dependent effect of the drug. A small reversible decrease of the baseline ratio is seen after the addition of pimozide. (d) Summary of responses obtained in arterioles exposed to pimozide ($n=4$) and in vehicle control experiments ($n=4$). *$P<0.05$, **$P<0.01$, and *** $P<0.001$; *t*-test vs untreated or vehicle control experiments.

Expression of α_1 and β calcium channel subunits

RNA was extracted from mesenteric arterioles of two rats and analyzed along with RNA obtained from various rat organs as positive controls. Amplification products for P- and Q-type calcium channels $Ca_V2.1a$ and $Ca_V2.1b$ were not detected in mesenteric arterioles with template cDNA from 0.5 mm vessel length and after amplification for up to 34 cycles. Amplification products were readily obtained for both P- and Q-type channels with 50 ng cerebral cortex cDNA as template (Figure 6). Sequencing of amplification products revealed 100% homology to the respective splice variant sequences for P- and Q-type calcium channel α_1-subunits. Previously reported expression in mesenteric arterioles of T-type channel α_1-subunit $Ca_V3.1$ (Gustafsson *et al*., 2001) was confirmed on the same cDNA batches using the same amount of starting cDNA (Figure 6).

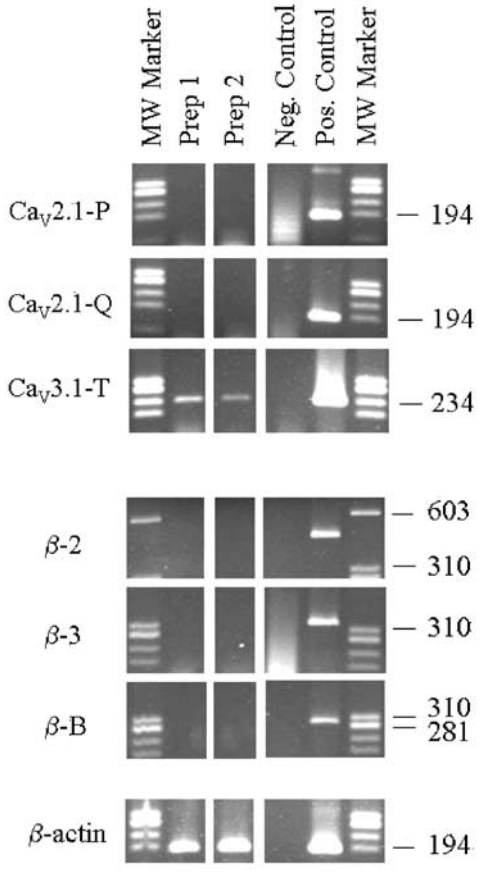

Figure 6 Agarose-gel electrophoresis showing PCR products obtained when using specific primers for selected α_1- and β-subunits of voltage-dependent Ca^{2+} channels and cDNA from mesenteric arterioles. The $Ca_V2.1$-P and $Ca_V2.1$-Q are alternative splice variants of the same gene and corresponds to the P-type and Q-type α_1-subunits, respectively. $Ca_V3.1$-T corresponds to the α_{1G}-subunit of T-type channels. β-2 (cardiac), β-3 (smooth muscle), and β-B (β_{1b}, neuronal) are known β-subunits of high-voltage-activated Ca^{2+} channels. Specific primer for β-actin was also included in the reactions. Pooled cDNA from mesenteric arterioles in each of two rats were used (Prep 1, Prep 2). Appropriate controls are shown in which cDNA was omitted (neg. control) or 50 ng template cDNA isolated from various rat organs (cerebral cortex, left cardiac ventricle, or renal inner medulla) was included in the PCR (pos. control).

We did not detect products for any of the tested β-subunits: neuronal β_{1b}, cardiac β_2, or neuronal/smooth muscle β_3 using cDNA corresponding to 0.5 mm vessel length as starting amount and 33 cycles of amplification (Figure 6). In each of the PCRs, significant amplification products were obtained in the positive controls (cerebral cortex, left cardiac ventricle, or renal inner medulla). When arteriolar cDNA was amplified for β-actin with intron-spanning primers, significant products were obtained at the correct size, indicating intact template and a cDNA origin of the amplification products. Amplification products were obtained only in the presence of cDNA in each of the RT–PCRs.

Discussion

We have measured intracellular Ca^{2+} in mesenteric small arterioles and provide evidence of a depolarization-activated influx pathway dominated by mibefradil-sensitive Ca^{2+} channels. The magnitude of the Ca^{2+} response to 75 mM extracellular K^+ was an increase to 108% of the baseline Fura-2 ratio (Figure 2b), corresponding to an increase in $[Ca^{2+}]_i$ from ~70 nM at rest to ~130 nM during sustained depolarization.

Basal characteristics of the KCl-induced Ca^{2+} response

The Ca^{2+} response to high-K^+ was strictly dependent on extracellular Ca^{2+}, arguing in favor of Ca^{2+} entry *via* plasma membrane channels. The ~60% inhibition of the response by $LaCl_3$ is another indication of the involvement of Ca^{2+} channels, since La^{3+} and other trivalent metal ions are known to inhibit voltage-dependent as well as voltage-independent Ca^{2+} entry pathways (Beedle *et al*., 2002; Jung *et al*., 2002).

To rule out that the preparation contained functional nerve endings we tested the effect of TTX, an inhibitor of voltage-dependent Na^+ channels, and phentolamine, a nonspecific α-adrenoceptor antagonist. As none of these substances had an effect on the response to 75 mM K^+ (Figure 2b), we concluded that the activation of α-adrenergic receptors *via* local neurotransmitter release did not play a role in the responses.

Since mibefradil inhibits both vasoconstriction of mesenteric arterioles *in vivo* (Gustafsson *et al*., 2001) and the nifedipine-insensitive Ca^{2+} current in isolated mesenteric VSMC (Morita *et al*., 2002), we conclude that Ca^{2+} channels are expressed in the arteriolar smooth muscle. However, based on our Ca^{2+} response data, we cannot exclude that the endothelial cells might also express mibefradil-sensitive Ca^{2+} channels. The current view is that endothelial cells do not express voltage-dependent Ca^{2+} channels (Domenighetti *et al*., 1998; Nilius & Droogmans, 2001), although the opposite has also been suggested (Vinet & Vargas, 1999; Wu *et al*., 2003).

Channel pharmacology and inhibitor specificity

In rat mesenteric arterioles ($<40\,\mu$m), a role for dihydropyridine-insensitive channels in both local and conducted vasomotor responses was suggested because 10 μM nifedipine or nimodipine had no effects, and because the L-type $Ca_V1.2$ α_1-subunit was not expressed at the mRNA level (Gustafsson *et al*., 2001). Surprisingly, we found an effect of 1 μM nifedipine on the Ca^{2+} response to 75 mM K^+. However, there was

no effect of 500 nM calciseptine on the Ca^{2+} response in mesenteric arterioles (Figure 4). The efficacy of 500 nM calciseptine was confirmed using rat renal afferent arterioles known to express L-type channels (Salomonsson & Arendshorst, 1999; Loutzenhiser & Loutzenhiser, 2000). Together with our previous finding that L-type channel message is not expressed in mesenteric arterioles (Gustafsson *et al*., 2001), these data suggest that the observed inhibition by nifedipine is a nonspecific effect.

At present, we cannot explain the discrepancy between the dihydropyridine insensitivity of vasoconstriction in mesenteric arterioles *in vivo* (Gustafsson *et al*., 2001) and our *in vitro* data, but there are several possible explanations. A 40% inhibition of the Ca^{2+} increase *in vivo* by nifedipine could be insufficient to block vasoconstriction. Furthermore, we cannot directly compare the results obtained *in vivo* (37°C) with those obtained *in vitro* (room temp.), especially because the stimulation mode was different in the two studies: in the previous study vasoconstriction was induced by locally applied current pulses, whereas in the present study Ca^{2+} influx was measured during sustained depolarization using high KCl.

The P- and Q-type inhibitor ω-agatoxin IVA (10 nM) inhibited the KCl-induced Ca^{2+} increase in rabbit afferent arterioles (Hansen *et al*., 2000) and has low interaction with N- or L-type Ca^{2+} channels when applied in nanomolar concentrations (Mintz *et al*., 1992; McDonough *et al*., 2002). Since we observed no inhibition at 100 nM (Figure 4), it is safe to conclude that the P/Q-type channel is absent in rat mesenteric arterioles. This is in line with the RT–PCR, which did not show amplification of message for the two splice variants of $Ca_V2.1$ (α_{1A}-subunit) corresponding to the P- or Q-type channel (Figure 6).

In nanomolar concentrations, the peptide neurotoxin ω-conotoxin MVIIA is a specific inhibitor of transiently expressed $Ca_V2.2$ (α_{1B}) N-type channels (Feng *et al*., 2001; 2003). Another peptide neurotoxin, SNX-482, inhibited $Ca_V2.3$ channels (α_{1E}, R-type) stably expressed in a mammalian cell line with an EC_{50} of 15–30 nM. At high concentration (500 nM), SNX-482 had no effects on L- or T-type currents, but some effect on N-type currents (Newcomb *et al*., 1998). Compared to the reported EC_{50} values, the concentrations of ω-conotoxin MVIIA (500 nM) or SNX-482 (100 nM) employed in the present study were high, and the lack of any effects (Figure 4) indicates that N- and R-type Ca^{2+} channels are not expressed in this microvessel.

The above results suggested that inhibitors of the T-type voltage-dependent Ca^{2+} channels might be effective. Mibefradil has been shown to block T-type channels with an IC_{50} of 100−300 nM (Mishra & Hermsmeyer, 1994; Martin *et al*., 2000; Hansen *et al*., 2001; Morita *et al*., 2002). In rat mesenteric small arterioles, mibefradil was indeed effective at all the concentrations tested when a special protocol designed for use-dependent drugs was applied (Figures 5a and b). In comparison with the IC_{50} values mentioned above, the use-dependent inhibition of 29% seen with 100 nM mibefradil (Figure 5b) indicates binding to a channel with T-type pharmacology.

Recent studies show use- or voltage-dependent block by mibefradil for both high- and low-voltage-activated Ca^{2+} channels (Bezprozvanny & Tsien, 1995; Arnoult *et al*., 1998; McDonough & Bean, 1998; Jimenez *et al*., 2000; Morita *et al*., 2002). We designed a stimulation protocol to be able to show use dependence of mibefradil. The concentration-dependent effect of mibefradil increased proportionally with the number of prior high-K^+ stimulations and was maximal at the fourth consecutive stimulation (Figure 5a). The effect was independent of the length of the preincubation period prior to stimulation.

Pimozide is another drug with use-dependent effects (Arnoult *et al*., 1998). Cloned T-type channels were blocked with EC_{50} values around 30–50 nM (Santi *et al*., 2002), whereas native channels were blocked with $EC_{50} \sim 500$ nM (Enyeart *et al*., 1993; Arnoult *et al*., 1998). In the present study, 500 nM pimozide inhibited 85% of the Ca^{2+} response to 75 mM K^+ (Figure 5c and d). Pimozide was previously shown to block L-type channels with an EC_{50} of 75 nM (Enyeart *et al*., 1990) and N- and P-type Ca^{2+} channels with an EC_{50} in the micromolar range (Sah & Bean, 1994). Although pimozide is a potent blocker of L-type channels, these channels are not expressed in mesenteric arterioles, indicating that it blocked a channel with T-type pharmacology.

Identification of T-type subunits in mesenteric arterioles

In a previous study, we detected RT–PCR amplification of the T-type $Ca_V3.1$ and $Ca_V3.2$ α_1-subunits in both mesenteric arteries and arterioles from the rat (Gustafsson *et al*., 2001), and in the present study $Ca_V3.1$ expression in mesenteric arterioles was confirmed (Figure 6). Owing to careful dissection of the arterioles used in RT–PCR experiments, it is unlikely that RNA of nonvascular origin, for example, from fibroblasts, have contaminated the RNA extracted. However, we cannot rule out that endothelial RNA might have contributed to the RT–PCR products, and it is therefore a possibility that $Ca_V3.1$ may be expressed in endothelial cells.

The T-type channel has not been purified and the exact subunit composition is therefore unknown (Hofmann *et al*., 1999; Perez-Reyes, 2003). It has been shown that α_1–β interactions within the high-voltage-activated Ca^{2+} channel complex are promiscuous with respect to subunit isoforms (Walker & De Waard, 1998), suggesting that several α_1–β combinations would be possible in mesenteric arterioles expressing two T-type α_1-subunits ($Ca_V3.1$ and $Ca_V3.2$) and an unknown diversity of β-subunits. In rat mesenteric arteries, Ca^{2+} channels with T-type pharmacology display higher 50% activation and inactivation voltages ($V_{0.5}$) compared to classical T-type channels (Morita *et al*., 2002). We were therefore interested in testing whether known β-subunits were coexpressed with the α_1-subunits and, thus, could modify channel properties. However, our RT–PCR showed no amplification of the neuronal β_{1b}, cardiac β_2, or neuronal/smooth muscle β_3 subunits (Figure 6). Mapping the expression of known β- or $\alpha_2\delta$-subunits would give a better understanding of possible subunit interactions in mesenteric arterioles and is an interesting subject for future investigation.

Biophysical characteristics of non-L-type channels in mesenteric resistance vessels

In VSMC from rat or guinea-pig mesenteric artery, nifedipine-insensitive Ca^{2+} currents with T-type pharmacology activated at −50 to −40 mV and peaked at −10 to 0 mV (Morita *et al*., 1999; 2002). In contrast, the three cloned T-type α_1-subunits ($Ca_V3.1$, $Ca_V3.2$, and $Ca_V3.3$) all have an activation threshold

at −70 mV and peak of *I–V* curve at −30 mV at physiological [Ca^{2+}] (Perez-Reyes, 2003). It has therefore been proposed that the high-voltage-activated nifedipine-insensitive Ca^{2+} channels in mesenteric arteries, although they display T-type pharmacology, do not belong to the T-type channels. However, native T-type currents in some peripheral tissues, including smooth muscle, display activation threshold and peak current at −50 and −10 mV, respectively (Perez-Reyes, 2003), and with our demonstration of channels with T-type pharmacology and mRNA expression profile (Gustafsson *et al*., 2001); we think that it will be important to investigate the expression profile of auxiliary subunits capable of modifying the function of Ca^{2+} channel α_1-subunits.

Both mesenteric nifedipine-insensitive Ca^{2+} channels (Morita *et al*., 2002) and cloned $Ca_V3.1$ and $Ca_V3.2$ T-type channels (Perez-Reyes, 2003) display fast inactivation kinetics ($\tau_{inact} = 10-30$ ms). This raises the question as to how mesenteric Ca^{2+} channels are able to sustain prolonged Ca^{2+} influx during high K^+. One possibility is through small window currents in the voltage range where steady-state activation and inactivation curves overlap (McDonald *et al*., 1994; Perez-Reyes, 2003). It has been reported that a T-type window current was responsible for a physiological, steady-state Ca^{2+} entry in human myoblasts (Bijlenga *et al*., 2000), and window currents in the V_m range from −50 to −20 mV were suggested to account for high-K^+-induced, nifedipine-insensitive Ca^{2+} entry and vasoconstriction in rat mesenteric artery (Morita *et al*., 1999; 2002; Itonaga *et al*., 2002; Inoue & Mori, 2003). In pressurized small arterioles (hamster cheek pouch) resting V_m measured *in vivo* was −35 mV (Welsh & Segal, 1998). Under physiological pressure, it is therefore likely that a window type Ca^{2+} current in mesenteric arterioles is either present or can be activated by small changes in V_m.

Different effects of high KCl in vitro *and* in vivo

The dihydropyridine-insensitive voltage-dependent Ca^{2+} channels involved in conducted vasoconstriction (Gustafsson *et al*., 2001) most likely correspond to the mibefradil-sensitive channels we characterize in the present study. However, while 75 mM K^+ induced a sustained Ca^{2+} increase *in vitro* in the present study, superfusing the mesentery with 75 mM K^+ did not induce vasoconstriction *in vivo* (Gustafsson *et al*., 2001). One explanation might be that *in vivo* the blood perfusion maintained [K^+] in the vicinity of VSMC below 75 mM, whereby the induced depolarization was not in the membrane potential range where a sufficient window current can be reached. Another possibility is that KCl induced a counter regulatory effect *in vivo*. A recent report states that exposing the perfused mesenteric bed of the rat to 70 mM K^+ leads to an intraluminal release of nitric oxide (NO) *via* a NO synthase-independent pathway (Mendizabal *et al*., 2000). Release of NO might counteract the Ca^{2+} increase in VSMC with the net effect being no diameter change.

In summary, a voltage-dependent Ca^{2+} channel with T-type pharmacology is responsible for depolarization-induced Ca^{2+} influx in mesenteric arterioles where the L-type Ca^{2+} channel is not expressed. The sustained Ca^{2+} entry through this channel is most likely due to a window current in a narrow membrane voltage range in depolarized VSMC.

Ms. Anni Salomonsson and Mr. Ian Godfrey are acknowledged for their skillful technical assistance. This project received financial support from The Danish Heart Association (Grant Nos. 22938 and 22977), the Danish Medical Research Council (Grant Nos. 22-01-0459 and 22-02-0263), and the Novo Nordisk Foundation (Grant No. 2003-11-28). Mibefradil was a kind gift from F. Hoffmann-La Roche Ltd, Basel, Switzerland.

References

ANDREASEN, D., JENSEN, B.L., HANSEN, P.B., KWON, T.H., NIELSEN, S. & SKØTT, O. (2000). The α_{1G}-subunit of a voltage-dependent Ca^{2+} channel is localized in rat distal nephron and collecting duct. *Am. J. Physiol. Renal Physiol.,* **279,** F997–1005.

ARNOULT, C., VILLAZ, M. & FLORMAN, H.M. (1998). Pharmacological properties of the T-type Ca^{2+} current of mouse spermatogenic cells. *Mol. Pharmacol.,* **53,** 1104–1111.

BEEDLE, A.M., HAMID, J. & ZAMPONI, G.W. (2002). Inhibition of transiently expressed low- and high-voltage-activated calcium channels by trivalent metal cations. *J. Membr. Biol.,* **187,** 225–238.

BEZPROZVANNY, I. & TSIEN, R.W. (1995). Voltage-dependent blockade of diverse types of voltage-gated Ca^{2+} channels expressed in *Xenopus* oocytes by the Ca^{2+} channel antagonist mibefradil (Ro 40-5967). *Mol. Pharmacol.,* **48,** 540–549.

BIJLENGA, P., LIU, J.H., ESPINOS, E., HAENGGELI, C.A., FISCHER-LOUGHEED, J., BADER, C.R. & BERNHEIM, L. (2000). T-type α1H Ca^{2+} channels are involved in Ca^{2+} signaling during terminal differentiation (fusion) of human myoblasts. *Proc. Natl. Acad. Sci. U.S.A.,* **97,** 7627–7632.

BOURINET, E., SOONG, T.W., SUTTON, K., SLAYMAKER, S., MATHEWS, E., MONTEIL, A., ZAMPONI, G.W., NARGEOT, J. & SNUTCH, T.P. (1999). Splicing of α_{1A} subunit gene generates phenotypic variants of P- and Q-type calcium channels. *Nat. Neurosci.,* **2,** 407–415.

DE WEILLE, J.R., SCHWEITZ, H., MAES, P., TARTAR, A. & LAZDUNSKI, M. (1991). Calciseptine, a peptide isolated from black mamba venom, is a specific blocker of the L-type calcium channel. *Proc. Natl. Acad. Sci. U.S.A.,* **88,** 2437–2440.

DOMENIGHETTI, A.A., BENY, J.L., CHABAUD, F. & FRIEDEN, M. (1998). An intercellular regenerative calcium wave in porcine coronary artery endothelial cells in primary culture. *J. Physiol.,* **513** (Part 1), 103–116.

ENYEART, J.J., DIRKSEN, R.T., SHARMA, V.K., WILLIFORD, D.J. & SHEU, S.S. (1990). Antipsychotic pimozide is a potent Ca^{2+} channel blocker in heart. *Mol. Pharmacol.,* **37,** 752–757.

ENYEART, J.J., MLINAR, B. & ENYEART, J.A. (1993). T-type Ca^{2+} channels are required for adrenocorticotropin-stimulated cortisol production by bovine adrenal zona fasciculata cells. *Mol. Endocrinol.,* **7,** 1031–1040.

FENG, Z.P., DOERING, C.J., WINKFEIN, R.J., BEEDLE, A.M., SPAFFORD, J.D. & ZAMPONI, G.W. (2003). Determinants of inhibition of transiently expressed voltage-gated calcium channels by ω-conotoxins GVIA and MVIIA. *J. Biol. Chem.,* **278,** 20171–20178.

FENG, Z.P., HAMID, J., DOERING, C., BOSEY, G.M., SNUTCH, T.P. & ZAMPONI, G.W. (2001). Residue Gly1326 of the N-type calcium channel α_{1B} subunit controls reversibility of ω-conotoxin GVIA and MVIIA block. *J. Biol. Chem.,* **276,** 15728–15735.

GRYNKIEWICZ, G., POENIE, M. & TSIEN, R.Y. (1985). A new generation of Ca^{2+} indicators with greatly improved fluorescence properties. *J. Biol. Chem.,* **260,** 3440–3450.

GUSTAFSSON, F., ANDREASEN, D., SALOMONSSON, M., JENSEN, B.L. & HOLSTEIN-RATHLOU, N. (2001). Conducted vasoconstriction in rat mesenteric arterioles: role for dihydropyridine-insensitive Ca^{2+} channels. *Am. J. Physiol. Heart Circ. Physiol.,* **280,** H582–H590.

HANSEN, P.B., JENSEN, B.L., ANDREASEN, D., FRIIS, U.G. & SKØTT, O. (2000). Vascular smooth muscle cells express the α_{1A} subunit of a P-/Q- type voltage-dependent Ca^{2+} Channel, and it is functionally important in renal afferent arterioles. *Circ. Res.,* **87,** 896–902.

HANSEN, P.B., JENSEN, B.L., ANDREASEN, D. & SKØTT, O. (2001). Differential expression of T- and L-type voltage-dependent calcium channels in renal resistance vessels. *Circ. Res.,* **89,** 630–638.

HOFMANN, F., LACINOVA, L. & KLUGBAUER, N. (1999). Voltage-dependent calcium channels: from structure to function. *Rev. Physiol. Biochem. Pharmacol.,* **139,** 33–87.

INOUE, R. & MORI, Y. (2003). New target molecules in the drug control of blood pressure and circulation. *Curr. Drug Targets Cardiovasc. Haematol. Disord.,* **3,** 59–72.

ITONAGA, Y., NAKAJIMA, T., MORITA, H., HANANO, T., MIYAUCHI, Y., ITO, Y. & INOUE, R. (2002). Contribution of nifedipine-insensitive voltage-dependent Ca^{2+} channel to diameter regulation in rabbit mesenteric artery. *Life Sci.,* **72,** 487–500.

JIMENEZ, C., BOURINET, E., LEURANGUER, V., RICHARD, S., SNUTCH, T.P. & NARGEOT, J. (2000). Determinants of voltage-dependent inactivation affect mibefradil block of calcium channels. *Neuropharmacology,* **39,** 1–10.

JUNG, S., STROTMANN, R., SCHULTZ, G. & PLANT, T.D. (2002). TRPC6 is a candidate channel involved in receptor-stimulated cation currents in A7r5 smooth muscle cells. *Am. J. Physiol. Cell Physiol.,* **282,** C347–C359.

LOUTZENHISER, K. & LOUTZENHISER, R. (2000). Angiotensin II-induced Ca^{2+} influx in renal afferent and efferent arterioles: differing roles of voltage-gated and store-operated Ca^{2+} entry. *Circ. Res.,* **87,** 551–557.

MARTIN, R.L., LEE, J.H., CRIBBS, L.L., PEREZ-REYES, E. & HANCK, D.A. (2000). Mibefradil block of cloned T-type calcium channels. *J. Pharmacol. Exp. Ther.,* **295,** 302–308.

MCDONALD, T.F., PELZER, S., TRAUTWEIN, W. & PELZER, D.J. (1994). Regulation and modulation of calcium channels in cardiac, skeletal, and smooth muscle cells. *Physiol Rev.,* **74,** 365–507.

MCDONOUGH, S.I. & BEAN, B.P. (1998). Mibefradil inhibition of T-type calcium channels in cerebellar purkinje neurons. *Mol. Pharmacol.,* **54,** 1080–1087.

MCDONOUGH, S.I., BOLAND, L.M., MINTZ, I.M. & BEAN, B.P. (2002). Interactions among toxins that inhibit N-type and P-type calcium channels. *J. Gen. Physiol.,* **119,** 313–328.

MENDIZABAL, V.E., POBLETE, I., LOMNICZI, A., RETTORI, V., HUIDOBRO-TORO, J.P. & ADLER-GRASCHINSKY, E. (2000). Nitric oxide synthase-independent release of nitric oxide induced by KCl in the perfused mesenteric bed of the rat. *Eur. J. Pharmacol.,* **409,** 85–91.

MINTZ, I.M., VENEMA, V.J., SWIDEREK, K.M., LEE, T.D., BEAN, B.P. & ADAMS, M.E. (1992). P-type calcium channels blocked by the spider toxin ω-Aga-IVA. *Nature,* **355,** 827–829.

MISHRA, S.K. & HERMSMEYER, K. (1994). Selective inhibition of T-type Ca^{2+} channels by Ro 40-5967. *Circ. Res.,* **75,** 144–148.

MORITA, H., COUSINS, H., ONOUE, H., ITO, Y. & INOUE, R. (1999). Predominant distribution of nifedipine-insensitive, high voltage-activated Ca^{2+} channels in the terminal mesenteric artery of guinea pig. *Circ. Res.,* **85,** 596–605.

MORITA, H., SHI, J., ITO, Y. & INOUE, R. (2002). T-channel-like pharmacological properties of high voltage-activated, nifedipine-insensitive Ca^{2+} currents in the rat terminal mesenteric artery. *Br. J. Pharmacol.,* **137,** 467–476.

NEWCOMB, R., SZOKE, B., PALMA, A., WANG, G., CHEN, X., HOPKINS, W., CONG, R., MILLER, J., URGE, L., TARCZY-HORNOCH, K., LOO, J.A., DOOLEY, D.J., NADASDI, L., TSIEN, R.W., LEMOS, J. & MILJANICH, G. (1998). Selective peptide antagonist of the class E calcium channel from the venom of the tarantula *Hysterocrates gigas*. *Biochemistry,* **37,** 15353–15362.

NILIUS, B. & DROOGMANS, G. (2001). Ion channels and their functional role in vascular endothelium. *Physiol. Rev.,* **81,** 1415–1459.

PEREZ-REYES, E. (2003). Molecular physiology of low-voltage-activated T-type calcium channels. *Physiol. Rev.,* **83,** 117–161.

SAH, D.W. & BEAN, B.P. (1994). Inhibition of P-type and N-type calcium channels by dopamine receptor antagonists. *Mol. Pharmacol.,* **45,** 84–92.

SALOMONSSON, M. & ARENDSHORST, W.J. (1999). Calcium recruitment in renal vasculature: NE effects on blood flow and cytosolic calcium concentration. *Am. J. Physiol.,* **276,** F700–F710.

SANTI, C.M., CAYABYAB, F.S., SUTTON, K.G., MCRORY, J.E., MEZEYOVA, J., HAMMING, K.S., PARKER, D., STEA, A. & SNUTCH, T.P. (2002). Differential inhibition of T-type calcium channels by neuroleptics. *J. Neurosci.,* **22,** 396–403.

VANBAVEL, E., SOROP, O., ANDREASEN, D., PFAFFENDORF, M. & JENSEN, B.L. (2002). Role of T-type calcium channels in myogenic tone of skeletal muscle resistance arteries. *Am. J. Physiol. Heart Circ. Physiol.,* **283,** H2239–H2243.

VINET, R. & VARGAS, F.F. (1999). L- and T-type voltage-gated Ca^{2+} currents in adrenal medulla endothelial cells. *Am. J. Physiol.,* **276,** H1313–H1322.

WALKER, D. & DE WAARD, M. (1998). Subunit interaction sites in voltage-dependent Ca^{2+} channels: role in channel function. *Trends Neurosci.,* **21,** 148–154.

WELSH, D.G. & SEGAL, S.S. (1998). Endothelial and smooth muscle cell conduction in arterioles controlling blood flow. *Am. J. Physiol.,* **274,** H178–H186.

WU, S., HAYNES Jr, J, TAYLOR, J.T., OBIAKO, B.O., STUBBS, J.R., LI, M. & STEVENS, T. (2003). $Ca_V3.1$ (α_{1G}) T-type Ca^{2+} channels mediate vaso-occlusion of sickled erythrocytes in lung microcirculation. *Circ. Res.,* **93,** 346–353.

(Received November 26, 2003
Revised April 10, 2004
Accepted April 16, 2004)